Electronic Supplementary Material (ESI) for Physical Chemistry Chemical Physics.

Electronic Supplementary Information

Very rapid electronic relaxation process in a highly conjugated Zn(II)porphyrin–[26]hexaphyrin–Zn(II)porphyrin hybrid tape

Sangsu Lee,[a] Hirotaka Mori,[b] Taegon Lee,[c] Manho Lim,*[c] Atsuhiro Osuka,*[b] and Dongho Kim*[a]

[a] *Spectroscopy Laboratory for Functional π-Electronic Systems and Department of Chemistry, Yonsei University, Seoul 120-749, Korea*

[b] *Department of Chemistry and Graduate School of Science, Kyoto University, Sakyo-ku, Kyoto 606-8502, Japan.*

[c] *Department of Chemistry and Chemistry Institute of Functional Materials, Pusan National University, Busan 609-735, Korea.*

Contents

1. Experimental Details

Sample Preparation

Toluene (HPLC grade), toluene-d_8 (with 99.96 atom % D) and 2-methyltetrahydrofuran (anhydrous, ≥ 99%, inhibitor-free) were purchased from Sigma Aldrich and used without further purification. All time-resolved experiments are measured in stationary state.

Steady-State Absorption.

Steady-state UV-Vis absorption spectra were recorded on a commercial spectrometer (Cary5000, Varian). All steady-state measurements were carried out by using a quartz cuvette with a path length of 1 cm at ambient temperatures.

Temperature Dependence Experiments.

For the temperature-dependent steady-state and time-resolved absorption studies, a temperature-controlled liquid nitrogen cryostat (Optistat DN, Oxford Instruments) was used. The temperatures were maintained to within ±0.05 K and allowed to equilibrate for 30 minutes before spectroscopic measurements. The results were controlled by comparison with measurements in a regular cuvette at room temperature, as possible.

Femtosecond Transient Absorption.

The femtosecond time-resolved transient absorption (fs-TA) spectrometer consists of an optical parametric amplifier (OPA; Palitra, Quantronix) pumped by a Ti:sapphire regenerative amplifier system (Integra-C, Quantronix) operating at 1 kHz repetition rate and an optical detection system. The generated OPA pulses have a pulsewidth of ~ 150 fs and an average power of 100 mW in the range 280-2700 nm, which are used as pump pulses. White light continuum (WLC) probe pulses were generated using a sapphire window (3 mm thick) by focusing a small portion of the fundamental 800 nm pulses which was picked off by a quartz plate before entering the OPA. The time delay between pump and probe beams was carefully controlled by making the pump beam travel along a variable optical delay (ILS250, Newport). Intensities of the spectrally dispersed WLC probe pulses are monitored by a High Speed spectrometer (Ultrafast Systems) for both visible and near-infrared measurements. To obtain the time-resolved transient absorption difference signal (ΔA) at a specific time, the pump pulses were chopped at 500 Hz and absorption spectra intensities were saved alternately with or without pump pulse. Typically, 4000 pulses excite the samples to obtain the fs-TA spectra at each delay time. The polarization angle between pump and probe beam was set at the magic angle (54.7°) using a Glan-laser polarizer with a half-wave retarder in order to prevent polarization-dependent signals. Cross-correlation fwhm in pump-probe experiments

was less than 200 fs and chirp of WLC probe pulses was measured to be 800 fs in the 450-1400 nm region. To minimize chirp, all reflection optics in the probe beam path and a quartz cell of 2 mm path length were used. After fs-TA experiments, the absorption spectra of all compounds were carefully examined to detect if there were artifacts due to degradation and photo-oxidation of samples. The three-dimensional data sets of ΔA versus time and wavelength were subjected to singular value decomposition and global fitting to obtain the kinetic time constants and their associated spectra using Surface Xplorer software (Ultrafast Systems).

Femtosecond Transient Absorption in the near-infrared region.

Two identical home-built optical parametric amplifiers (OPA), pumped by a commercial Ti:sapphire regenerative amplifier (Hurricane, Spectra Physics) with a repetition rate of 1 kHz, are used to generate near IR pulses. Either signal (wavelength < 1600 nm) or idler (wavelength > 1600 nm) pulses of each OPA was selected by a dichroic mirror and served as a pump or a probe. Energy of pump pulse was kept less than 0.5 μJ and that of probe pulse < 10 nJ. The polarization of the pump pulse was set at the magic angle (54.7) relative to the probe pulse to recover the isotropic absorption spectrum. The broadband transmitted probe pulse was detected with a N_2(l)-cooled HgCdTe detector. The pump spot was made sufficiently larger than the probe spot to ensure spatially uniform photoexcitation across the spatial dimensions of the probe pulse. The instrument response function was typically ~150 fs.

2. Theoretical Calculations

The quantum calculations were performed using the supercomputing resources of the Korea Institute of Science and Technology Information (KISTI).[1] Geometry optimizations were carried out by the density functional theory (DFT) method with a new hybrid exchange–correlation functional using the coulomb-attenuating method,[2] employing a basis set containing 6-31G(d) for all atoms.[3] The X-ray crystallographic structures were used as initial geometries for geometry optimization.[4] To simulate the ground-state absorption spectra, we used time-dependent (TD) DFT calculations with the same functional and basis set as used in the geometry optimization.[5] All computational analyses were carried out omitting tertiary-butyl substituents and pentafluorophenyl in all phenyl groups to reduce computational cost since substituent effects on electronic structures of porphyrin rings by additional substituents far from porphyrin skeleton usually negligible.

3. Supporting Information

Table S1 Calculated vertical excitation energies of **FZn** at cam-B3LYP/6-31G(d) level.

No.	Energy (cm^{-1})	Wavelength (nm)	Osc. Strength	Major contributions	Minor contributions
1	6170.991	1620.485	0.75	H-1->L+1 (11%), HOMO->LUMO (82%)	H-3->L+2 (3%), HOMO->L+1 (4%)
2	7709.907	1297.032	0.0058	H-1->LUMO (81%), HOMO->L+1 (13%)	H-2->L+2 (3%), HOMO->LUMO (2%)
3	12170.99	821.6258	0	H-2->LUMO (67%), H-1->L+2 (16%)	H-4->L+2 (3%), HOMO->L+2 (7%)
4	13235.65	755.5353	0.3215	H-4->LUMO (21%), H-1->LUMO (10%), HOMO->L+1 (52%)	H-2->L+2 (5%), HOMO->LUMO (2%), HOMO->L+4 (3%)
5	13750.23	727.2603	0	H-3->LUMO (40%), HOMO->L+2 (31%)	H-6->LUMO (3%), H-2->L+1 (4%), H-2->L+4 (3%), H-1->L+3 (4%)
6	16026.35	623.9725	0	H-3->LUMO (37%), HOMO->L+2 (48%)	H-5->L+2 (3%), H-2->LUMO (6%)
7	16613.52	601.9193	0.7315	H-4->LUMO (39%), HOMO->L+1 (22%), HOMO->L+4 (10%)	H-5->LUMO (3%), H-3->L+3 (7%), H-2->L+2 (5%), H-1->LUMO (3%), H-1->L+1 (3%)
8	16867.59	592.8529	0.6626	H-5->LUMO (30%), H-1->L+1 (19%)	H-7->LUMO (3%), H-4->L+1 (7%), H-3->L+2 (8%), H-2->L+3 (4%), H-1->L+4 (6%), HOMO->LUMO (2%), HOMO->L+1 (5%), HOMO->L+4 (4%), HOMO->L+5 (8%)
9	18615.4	537.1895	3.7196	H-2->L+3 (10%), H-1->L+1 (56%), HOMO->LUMO (11%)	H-5->LUMO (8%), H-4->L+4 (4%), H-3->L+2 (3%), H-1->L+4 (3%)
10	18844.47	530.6597	0	H-1->L+2 (42%), HOMO->L+3 (16%)	H-8->LUMO (3%), H-6->LUMO (3%), H-4->L+2 (7%), H-3->L+1 (8%), H-3->L+4 (3%), H-2->LUMO (4%)
11	19351.79	516.748	0	H-2->LUMO (11%), H-1->L+2 (24%), HOMO->L+3 (35%)	H-6->LUMO (6%), H-3->LUMO (4%), H-3->L+4 (6%), H-2->L+5 (5%)
12	20852	479.5704	0	H-6->LUMO (48%)	H-8->LUMO (8%), H-7->L+2 (5%), H-5->L+2 (5%), H-4->L+3 (4%), H-2->L+4 (8%), H-1->L+3 (6%), HOMO->L+3 (8%)
13	21139.94	473.0383	0.3408	H-7->LUMO (28%), H-5->LUMO (21%), H-4->LUMO (10%), HOMO->L+4 (14%)	H-6->L+2 (6%), HOMO->L+1 (3%), HOMO->L+5 (8%)
14	21397.23	467.3502	0.2355	H-7->LUMO (10%), H-4->LUMO (23%), HOMO->L+4 (24%), HOMO->L+5 (11%)	H-6->L+2 (3%), H-5->LUMO (6%), H-3->L+3 (3%), H-2->L+2 (7%), H-1->L+5 (4%)
15	21861.81	457.4187	0.0332	H-7->LUMO (34%), H-5->LUMO (13%), HOMO->L+5 (19%)	H-10->LUMO (5%), H-4->L+4 (2%), H-2->L+3 (6%), H-1->L+4 (5%)
16	22768.38	439.2056	0	H-8->LUMO (32%), H-3->L+1 (35%)	H-11->LUMO (7%), H-6->LUMO (5%), H-6->L+1 (3%), H-2->L+1 (5%)
17	23477.35	425.9425	0	H-6->LUMO (11%), H-2->L+1 (38%), H-1->L+3 (10%)	H-4->L+3 (5%), H-3->LUMO (9%), H-3->L+1 (3%), H-2->L+4 (6%), HOMO->L+2 (7%), HOMO->L+6 (3%)
18	23498.32	425.5624	0.5717	H-10->LUMO (53%), HOMO->L+5 (19%)	H-10->L+5 (3%), H-7->LUMO (3%), H-3->L+2 (2%), H-2->L+3 (2%), H-1->L+4 (3%)
19	23945.15	417.621	0	H-8->LUMO (16%), H-2->L+1 (32%)	H-14->LUMO (3%), H-11->LUMO (3%), H-6->LUMO (3%), H-3->L+1 (6%), H-2->L+4 (7%), H-1->L+3 (6%), HOMO->L+3 (8%)
20	24250.03	412.3706	0	H-3->L+1 (28%), HOMO->L+3 (17%)	H-8->LUMO (7%), H-6->LUMO (5%), H-5->L+3 (3%), H-4->L+2 (4%), H-2->L+1 (8%), H-2->L+4 (5%), H-1->L+2 (3%), H-1->L+3 (3%), HOMO->L+7 (3%)

Table S2 Calculated vertical excitation energies of **HZn** at cam-B3LYP/6-31G(d) level.

No.	Energy (cm^{-1})	Wavelength (nm)	Osc. Strength	Major contributions	Minor contributions
1	9594.838	1042.227	0.0868	H-1->L+1 (27%), HOMO->LUMO (66%)	H-3->L+1 (6%), HOMO->L+1 (2%)
2	12022.58	831.768	0.0143	H-1->LUMO (49%), HOMO->L+1 (38%)	H-3->LUMO (8%), HOMO->LUMO (3%)
3	19246.13	519.5848	0	H-5->L+2 (20%), H-4->L+3 (19%), H-3->L+4 (15%), H-2->L+5 (20%)	H-2->L+1 (4%), H-2->L+3 (2%), H-1->L+4 (8%)
4	19264.69	519.0845	0.0086	H-5->L+3 (20%), H-4->L+2 (20%), H-3->L+5 (14%), H-2->L+4 (23%)	H-3->L+1 (3%), H-1->L+5 (8%)
5	19274.36	518.8239	0	H-5->L+4 (18%), H-4->L+5 (17%), H-3->L+2 (16%), H-2->L+3 (23%)	H-4->L+1 (3%), H-4->L+3 (2%), H-2->LUMO (2%), H-2->L+5 (2%), H-1->L+2 (9%)
6	19284.85	518.5418	0.0176	H-5->L+5 (17%), H-4->L+4 (19%), H-3->L+3 (16%), H-2->L+2 (25%)	H-5->L+1 (3%), H-1->L+3 (9%)
7	20425.33	489.5883	1.4488	H-1->LUMO (40%), H-1->L+1 (11%), HOMO->L+1 (30%)	H-7->LUMO (2%), H-3->LUMO (8%), HOMO->LUMO (7%)
8	20480.17	488.2772	2.6882	H-1->LUMO (10%), H-1->L+1 (48%), HOMO->LUMO (20%), HOMO->L+1 (10%)	H-7->LUMO (5%), H-5->LUMO (3%)
9	21073.8	474.5229	0	H-2->LUMO (91%)	
10	21708.56	460.6477	0	H-4->LUMO (92%)	
11	21819.87	458.2979	0.0705	H-5->LUMO (83%)	H-7->LUMO (2%), H-3->LUMO (4%), H-1->L+1 (2%)
12	21942.46	455.7373	0.327	H-3->LUMO (72%), HOMO->L+1 (21%)	H-5->LUMO (4%)
13	24227.45	412.755	0	H-2->L+1 (91%)	H-2->L+5 (2%)
14	24455.71	408.9025	0.1555	H-7->LUMO (19%), H-3->L+1 (63%), H-1->L+1 (10%)	
15	24803.33	403.1716	0	H-6->LUMO (10%), H-4->L+1 (80%)	
16	24967.87	400.5147	0.0571	H-5->L+1 (88%)	
17	25291.3	395.3929	0	H-6->LUMO (52%), H-4->L+1 (12%)	H-19->LUMO (4%), H-8->LUMO (3%), H-8->L+1 (3%), H-7->L+6 (2%), HOMO->L+2 (4%), HOMO->L+4 (3%), HOMO->L+6 (7%)
18	25294.53	395.3424	1.2916	H-7->LUMO (45%), H-3->L+1 (16%), HOMO->L+3 (21%)	H-5->L+1 (3%), H-2->L+4 (2%), H-1->L+5 (2%), HOMO->LUMO (3%)
19	25604.25	390.5602	0	HOMO->L+2 (87%)	H-6->LUMO (2%)
20	25778.46	387.9207	0.3886	H-7->LUMO (15%), HOMO->L+3 (71%)	H-5->L+3 (2%), H-3->L+1 (4%)

Table S3 Amplitudes of the fitted decay components in the excitation wavelength dependent TA decay profiles of **FZn** in toluene containing 1% pyridine.

	λ_{pump} = 420 nm		λ_{pump} = 470 nm		λ_{pump} = 540 nm		λ_{pump} = 630 nm		λ_{pump} = 760 nm		λ_{pump} = 1300 nm	
λ_{probe} (nm)	875	1100	875	1100	875	1100	875	1100	875	1100	875	1100
τ_1 (%)	66	85	75	88	77	90	81	92	81	92	85	95
τ_2 (%)	34	15	25	12	23	10	19	8	19	8	15	5

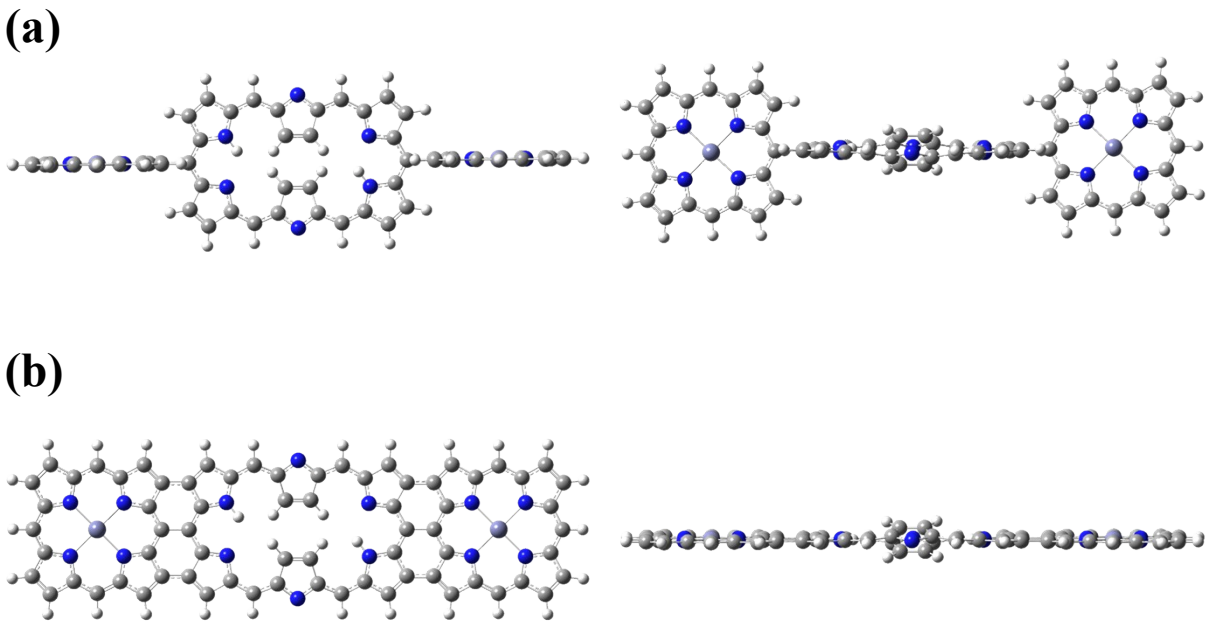

Fig. S1 Calculated molecular structures of (a) **HZn** and (b) **FZn** at cam-B3LYP/6-31G(d) level with top (left) and side view (right).

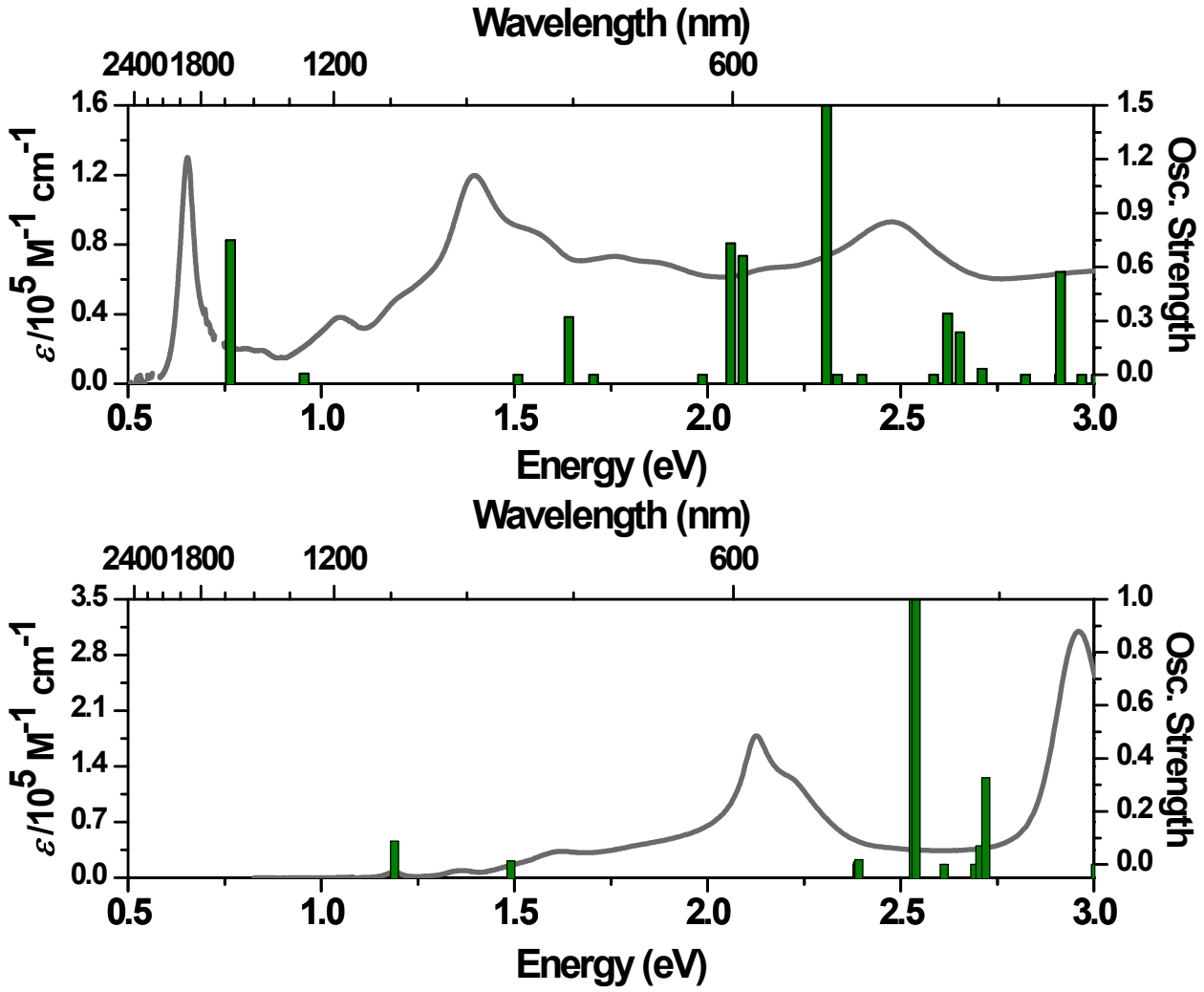

Fig. S2 Calculated vertical excitation energies based on the optimized structures (green bars) and measured absorption spectra (gray line) of **FZn** (top) and **HZn** (bottom).

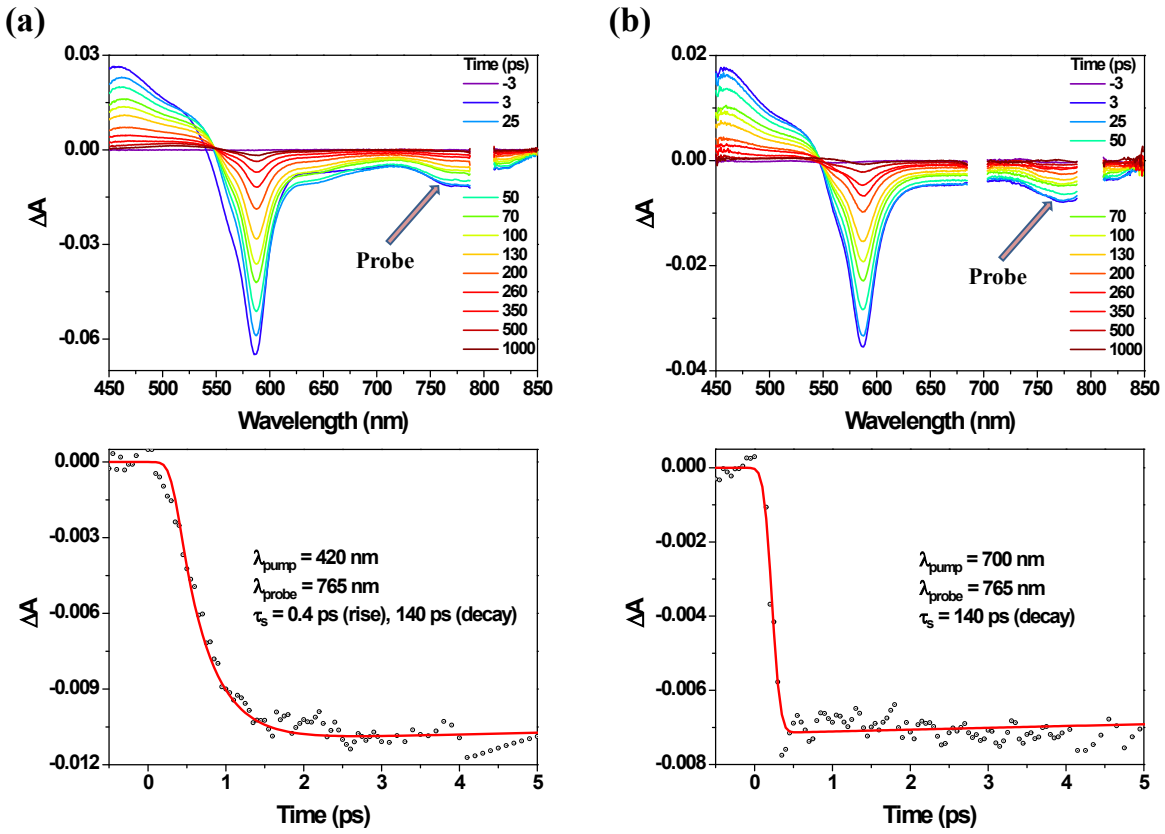

Fig. S3 Femtosecond transient absorption spectra of **HZn** (top) in toluene and decay profiles (bottom) with the photoexcitation at (a) 420 and (b) 700 nm.

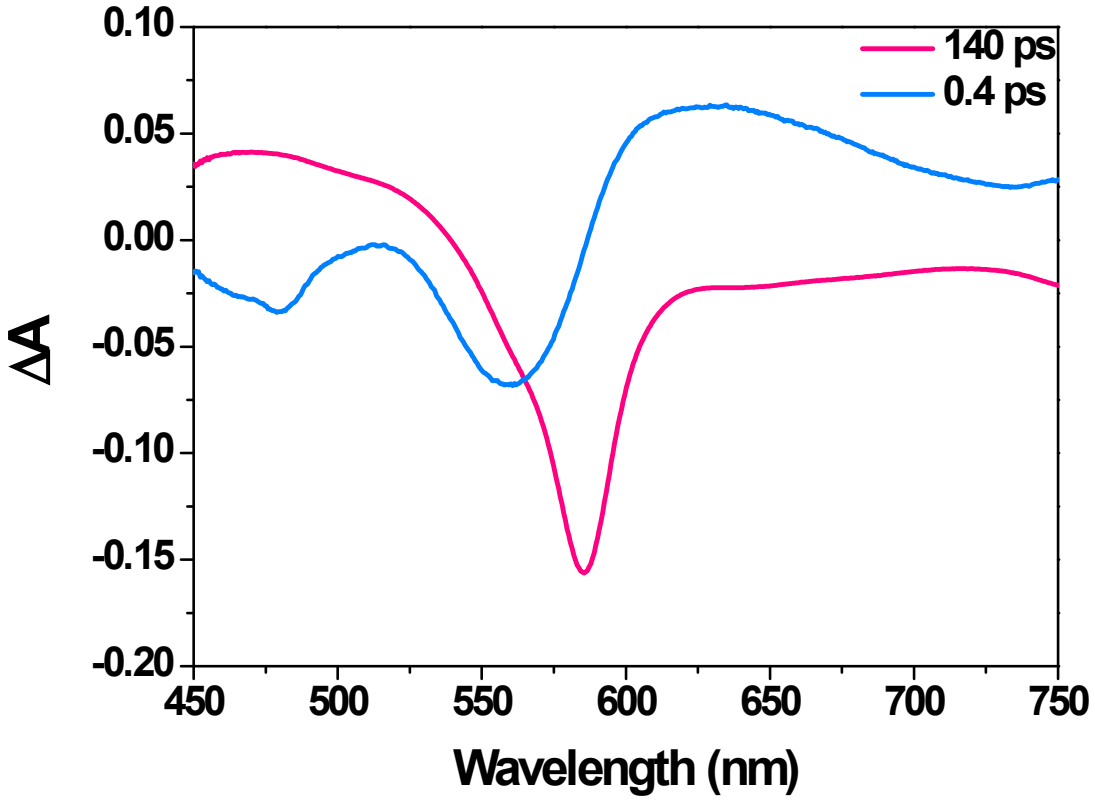

Fig. S4 Decay associated spectra of **HZn** upon photoexcitation at 420 nm obtained by global analysis.

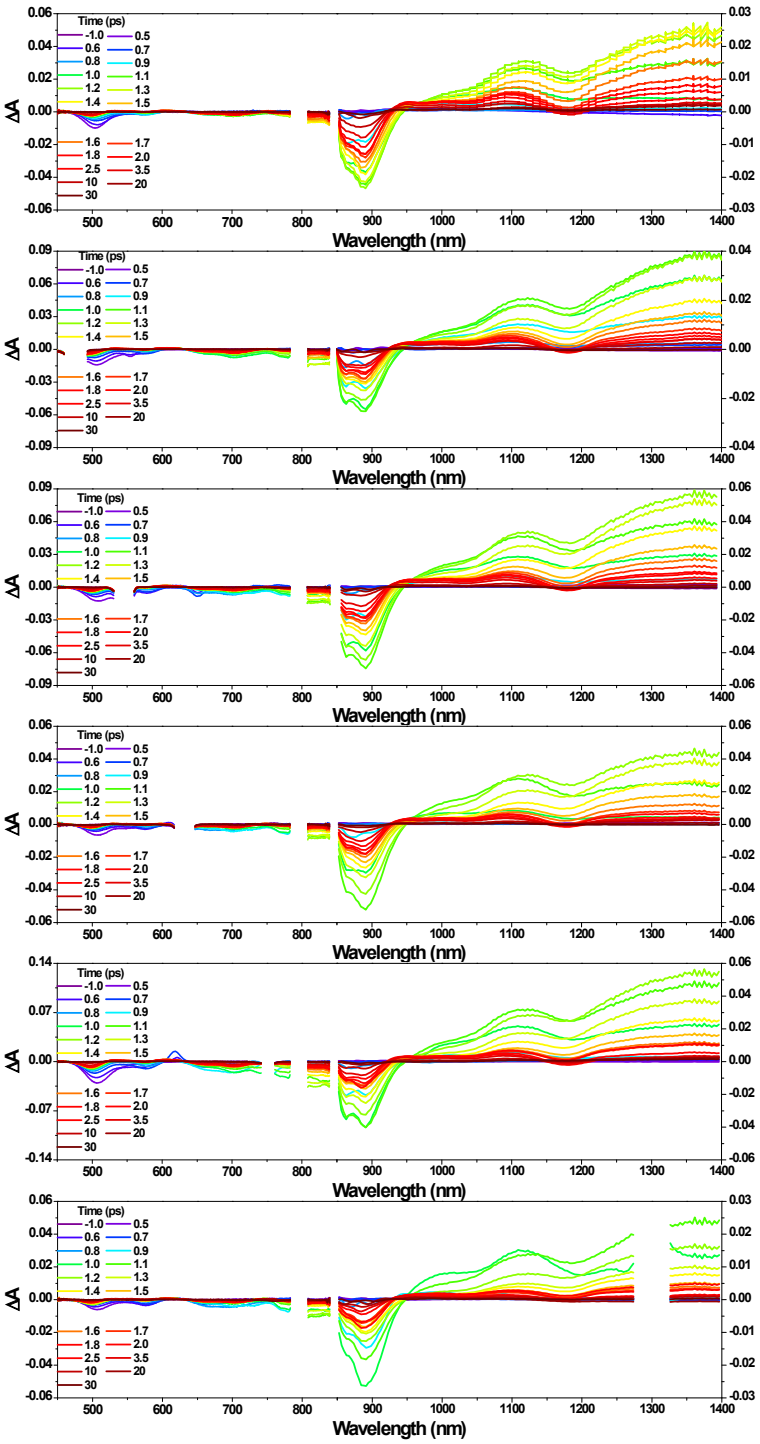

Fig. S5 Femtosecond transient absorption spectra of **FZn** in toluene containing 1% pyridine obtained with the photoexcitation at 420, 470, 540, 630, 760 and 1300 nm from top to bottom.

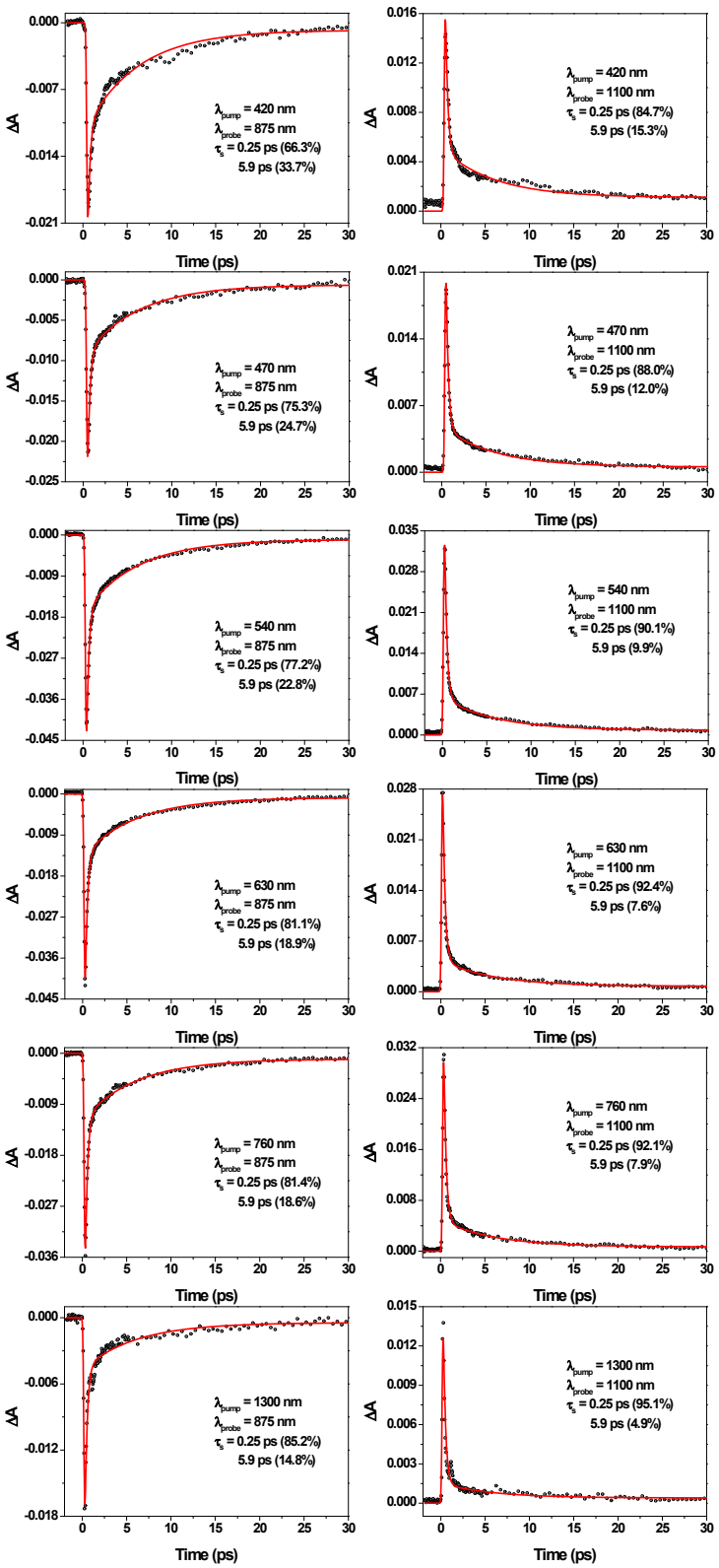

Fig. S6 Decay profiles of **FZn** in toluene containing 1% pyridine obtained with the photoexcitation at 420, 470, 540, 630, 760 and 1300 nm from top to bottom.

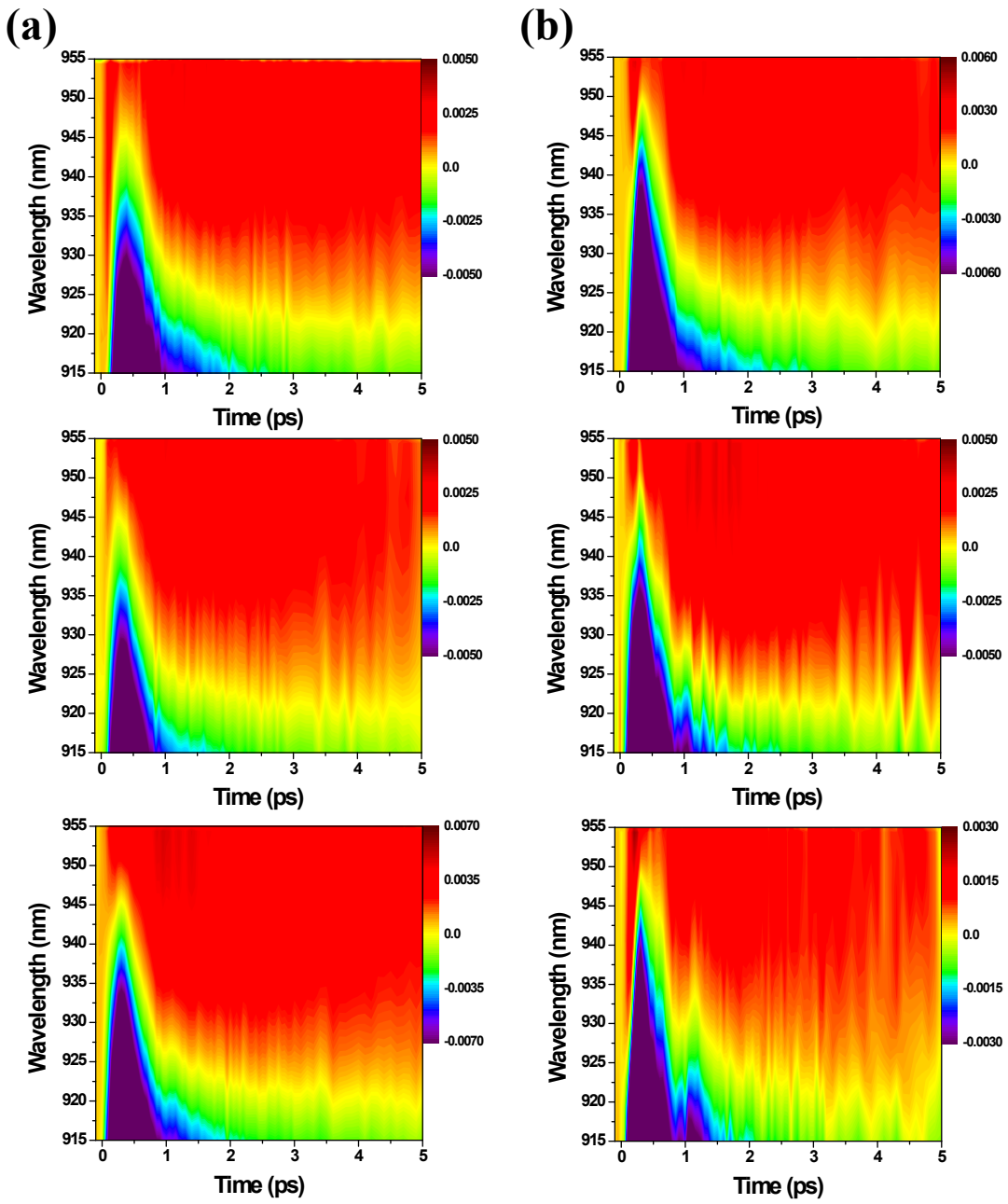

Fig. S7 Two-dimensional TA contour map of **FZn** in toluene containing 1% pyridine with photoexcitation at (a) 420 (top), 470 (middle) and 540 nm (bottom), (b) 630 (top), 760 (middle) and 1300 nm (bottom). The color scale represents the transient absorption signals (ΔA). Thus, the crossing points (ΔA=0) between excited-state absorption and ground-state bleaching spectra are represented by yellow color.

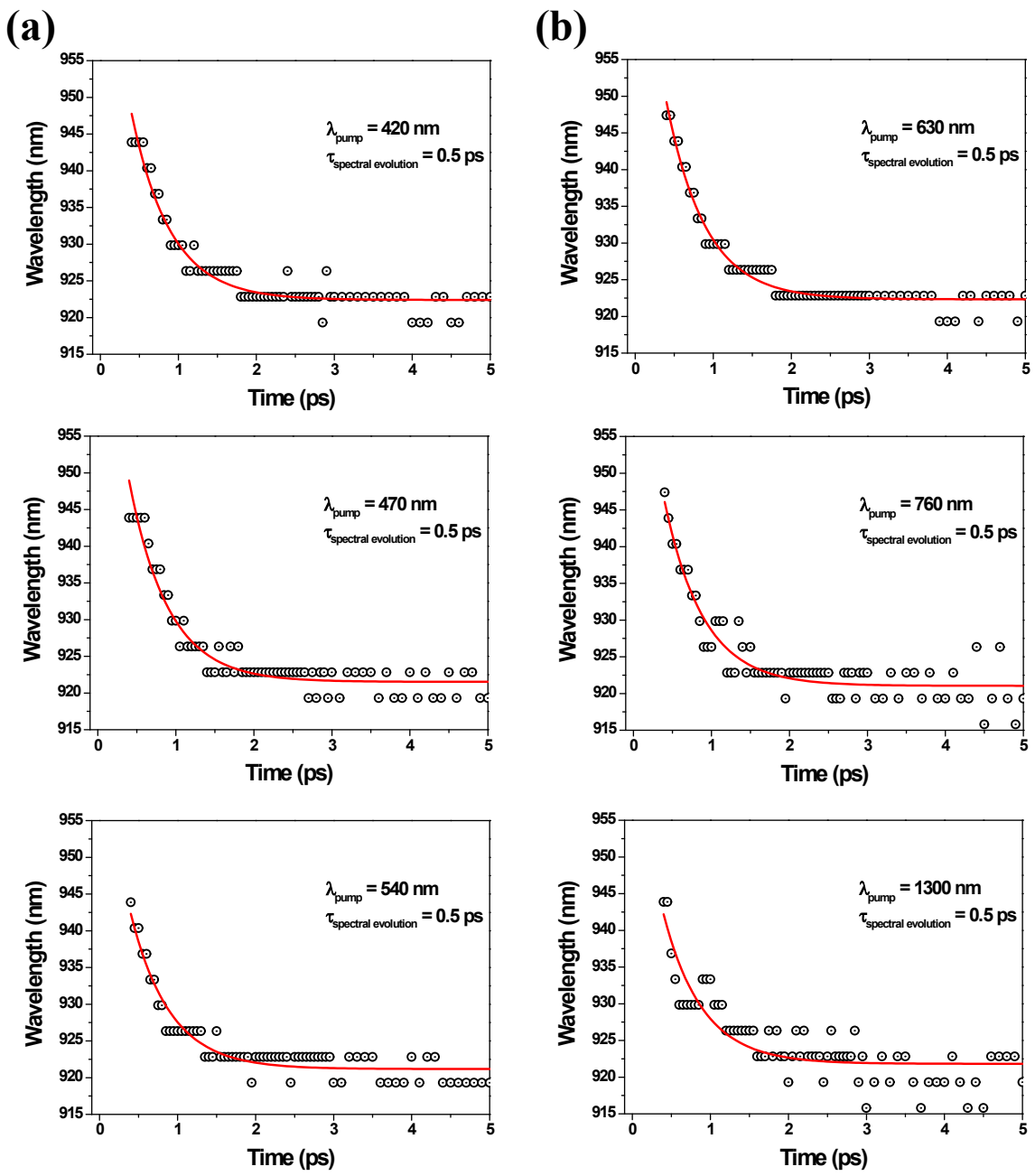

Fig. S8 Spectral evolutions (ΔA=0) of **FZn** in toluene containing 1% pyridine with the photoexcitation at (a) 420 (top), 470 (middle) and 540 nm (bottom), (b) 630 (top), 760 (middle) and 1300 nm (bottom).

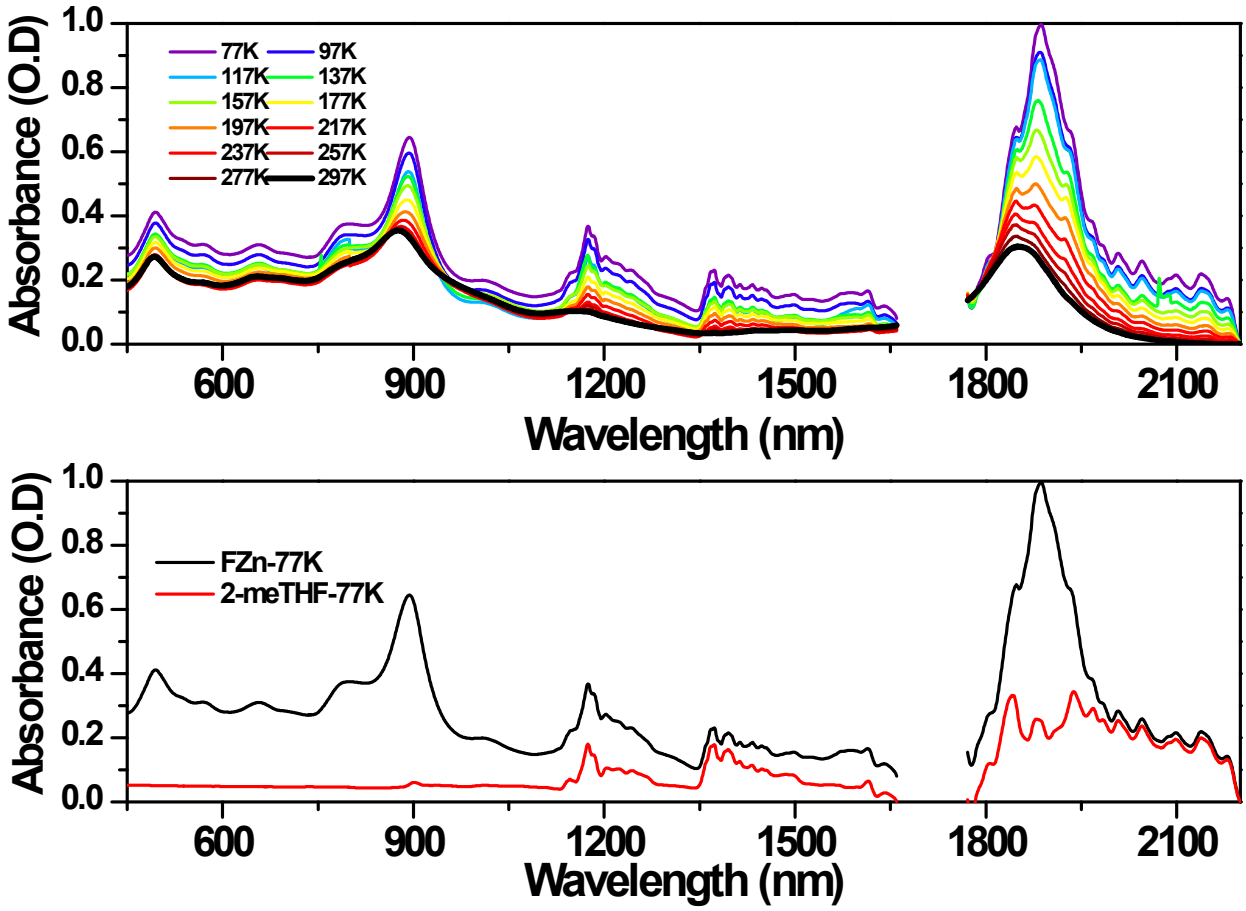

Fig. S9 Temperature-dependent steady-state absorption spectra of **FZn** in 2-meTHF (top) and in comparison with the absorption of pure 2-meTHF at 77K (bottom).

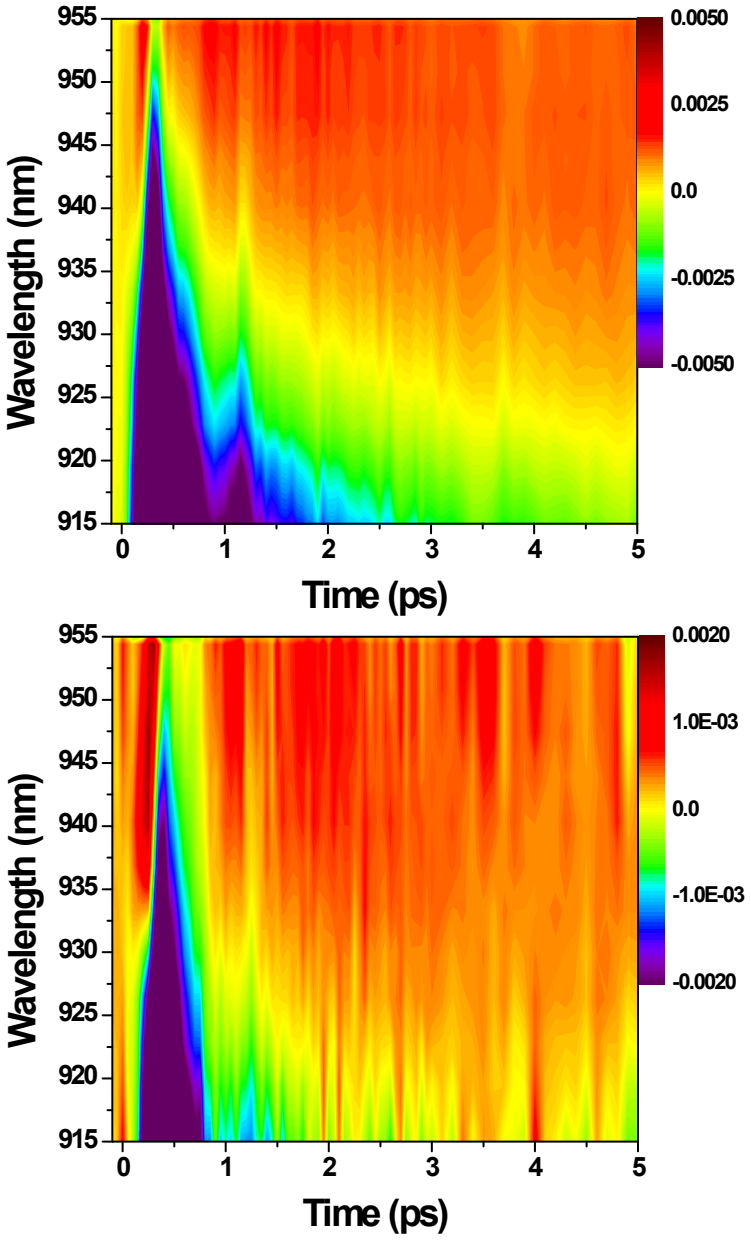

Fig. S10 Femtosecond transient absorption spectra of **FZn** in 2-meTHF obtained with the photoexcitation at 1300 nm at 77 (top) and 297 K (bottom). The color scale represents the transient absorption signals (ΔA). Thus, the crossing points (ΔA=0) between excited-state absorption and ground-state bleaching spectra are represented by yellow color.

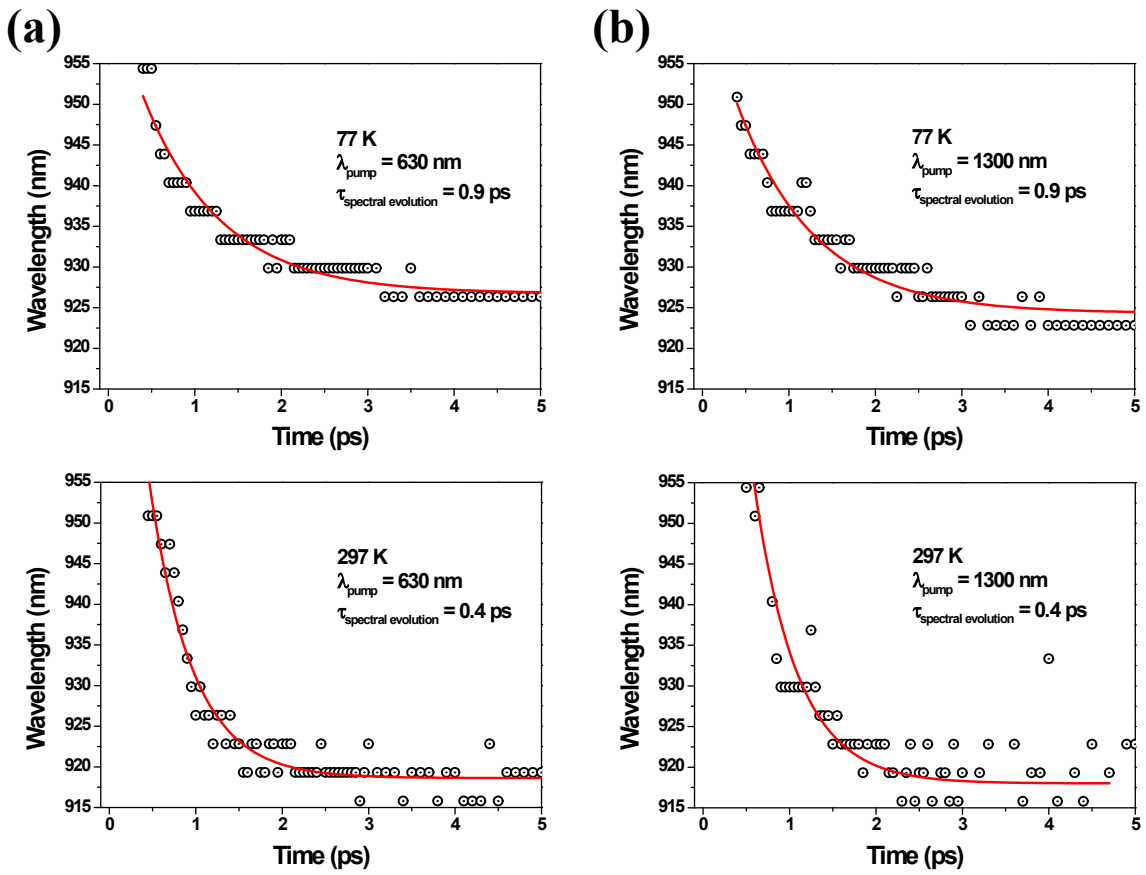

Fig. S11 Spectral evolutions (ΔA=0) of **FZn** in 2-meTHF with the photoexcitation at (a) 630 nm at 77 (top) and 297 K (bottom) and (b) 1300 nm at 77 (top) and 297 K (bottom).

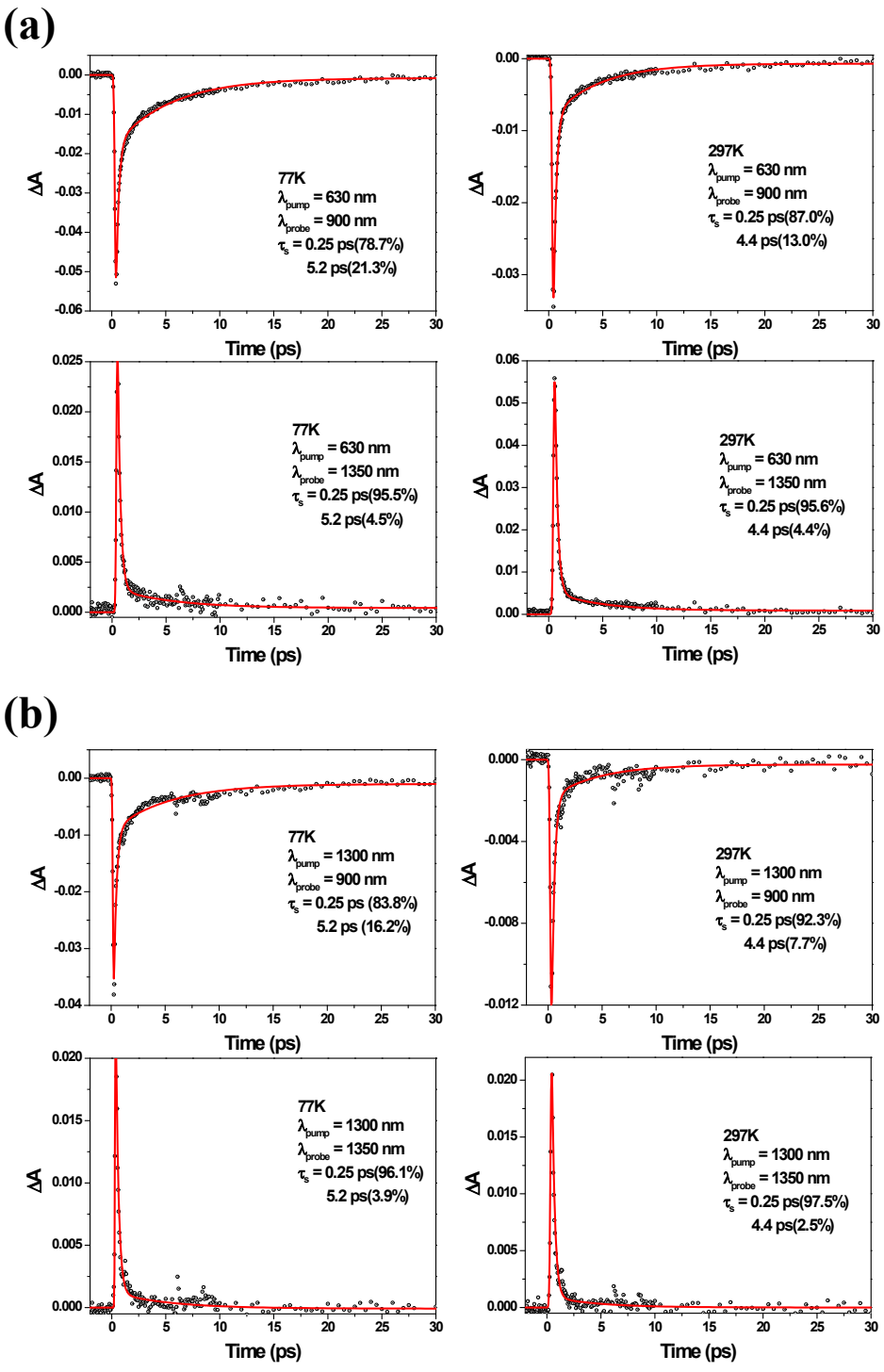

Fig S12. Decay profiles of **FZn** in 2-meTHF obtained with the photoexcitation at (a) 630 nm at 77 (left) and 297 K (right) and (b) 1300 nm at 77 (left) and 297 K (right).

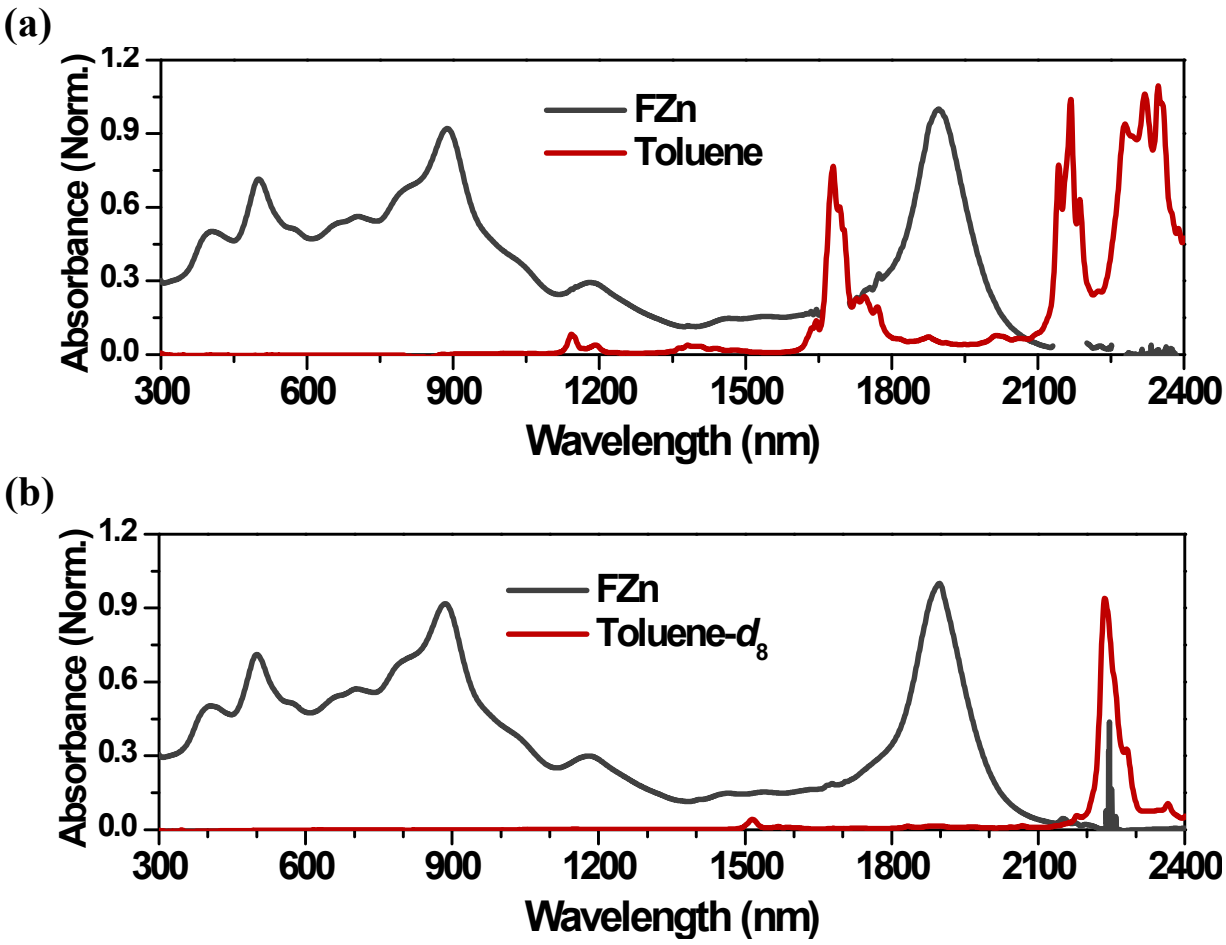

Fig. S13 (a) Absorption spectra of **FZn** in toluene containing 1% pyridine (black) and pure toluene (red). (b) Absorption spectra of **FZn** in toluene-d_8 containing 1% pyridine (black) and pure toluene-d_8 (red).

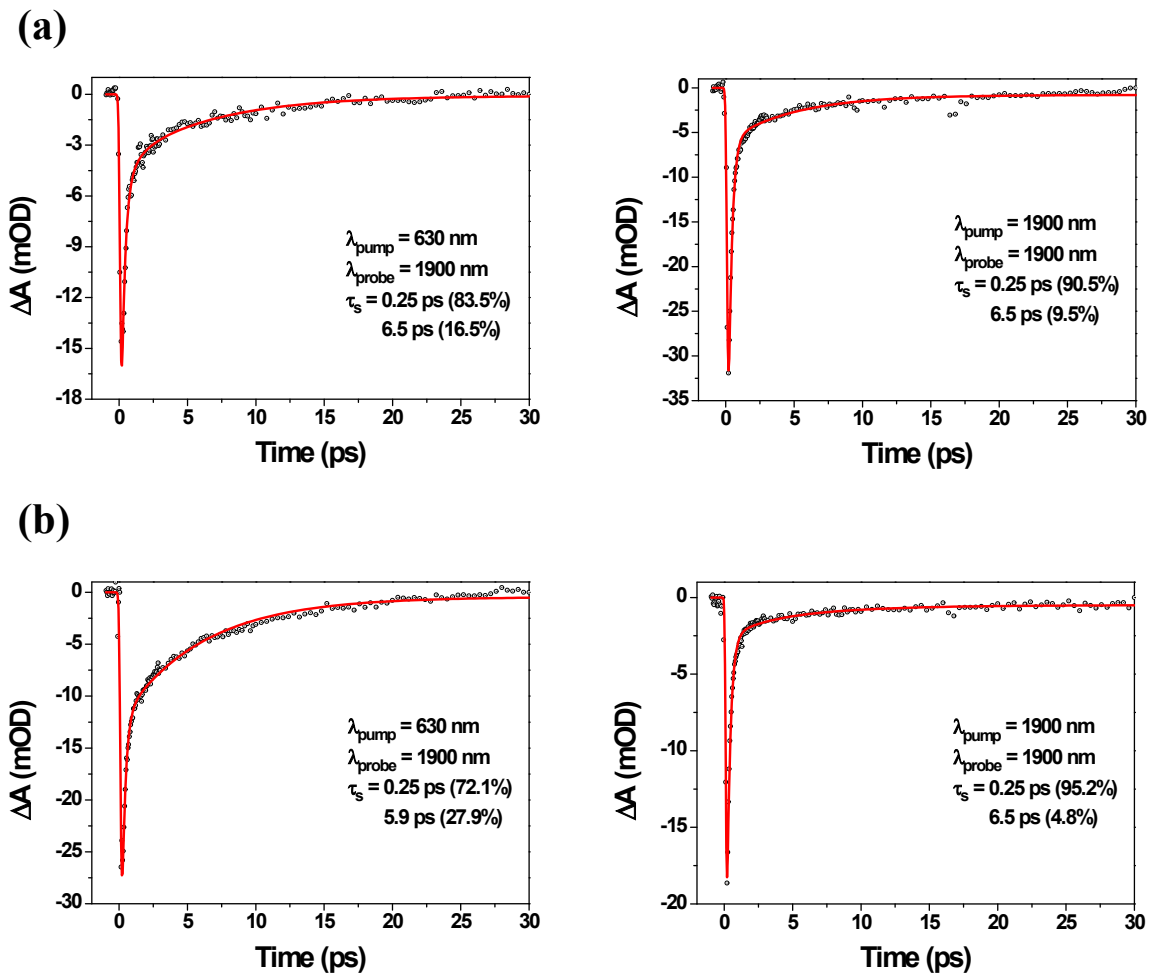

Fig. S14 (a) Decay profile of **FZn** in toluene-d_8 containing 1% pyridine obtained with photoexcitation at 630 (left) and 1900 nm (right). (b) Decay profile of **FZn** in toluene containing 1% pyridine obtained with photoexcitation at 630 (left) and 1900 nm (right).

4. References

1. M. J. Frisch, G. W. Trucks, H. B. Schlegel, G. E. Scuseria, M. A. Robb, J. R. Cheeseman, V. G. Zakrzewski, J. A. J. Montgomery, R. E. Stratmann, J. C. Burant, S. Dapprich, J. M. Millam, A. D. Daniels, K. N. Kudin, M. C. Strain, O. Farkas, J. Tomasi, V. Barone, M. Cossi, R. Cammi, B. Mennucci, C. Pomelli, C. Adamo, S. Clifford, J. Ochterski, G. A. Petersson, P. Y. Ayala, Q. Cui, K. Morokuma, D. K. Malick, A. D. Rabuck, K. Raghavachari, J. B. Foresman, J. Cioslowski, J. V. Ortiz, B. B. Stefanov, G. Liu, A. Liashenko, P. Piskorz, I. Komaromi, R. Gomperts, R. L. Martin, D. J. Fox, T. Keith, M. A. Al-Laham, C. Y. Peng, A. Nanayakkara, C. Gonzalez, M. Challacombe, P. M. W. Gill, B. G. Johnson, W. Chen, M. W. Wong, J. L. Andres, M. Head-Gordon, E. S. Replogle and J. A. Pople, Gaussian, Inc., Wallingford CT, 2004.
2. T. Yanai, D. P. Tew and N. C. Handy, *Chem. Phys. Lett.,* 2004,**393**, 51-57.
3. R. Ditchfield, W. J. Hehre and J. A. Pople, *J. Chem. Phys.,* 1971, **54**, 724-728.
4. H. Mori, T. Tanaka, S. Lee, J. M. Lim, D. Kim and A. Osuka, *J. Am. Chem. Soc*., 2015, **137**, 2097−2106
5. R. Bauernschmitt and R. Ahlrichs, *Chem. Phys. Lett.,* 1996, **256**, 454-464.